BETA-DECAY HALF-LIFE UNCERTAINTY OF THE EXTREMELY NEUTRON-RICH NUCLEI DUE TO NUCLEAR-MASS DEVIATION

Nguyen Duy Ly[†]

Faculty of Fundamental Sciences, Van Lang University
69/68 Dang Thuy Tram Street, Ward 13, Binh Thanh District
Ho Chi Minh City 700000, Vietnam

Nguyen Ngoc Duy[‡]

Institute of Postgraduate Education, Van Lang University
69/68 Dang Thuy Tram Street, Ward 13, Binh Thanh District
Ho Chi Minh City 700000, Vietnam

Nguyen Kim Uyen

Department of Physics, Sungkyunkwan University, Suwon 16419, South Korea

Le Hong Khiem

Institute of Physics, Vietnam Academy of Science and Technology
Hanoi 10000, Vietnam
and
Graduate University of Science and Technology
Vietnam Academy of Science and Technology, Hanoi 10000, Vietnam

Received 14 March 2023, accepted 29 August 2023, published online 7 September 2023

The beta-decay rates of neutron-rich nuclei far from the stability are still very limited due to the lack of experimental data. In this paper, we calculated the half-lives of the exotic nuclei close to the neutron drip line by using a recent semi-empirical formula ($F_{\rm Zh}$). The β-decay Q-values calculated using the finite-range droplet macroscopic (FRDM) model and taken from the AME2020 database (with and without uncertainty) were used in the calculations to investigate the impact of the mass uncertainty on the half-life predictions. We found that a deviation of 7% in the Q-value can lead to an uncertainty of 40% in the half-life and a large change, up to two orders of magnitude, in the r-process abundance. The approach combining the AME2020 Q-value and $F_{\rm Zh}$ model has emerged as a good tool for the half-life prediction. The estimated half-lives are necessary for the precise mass measurements and r-process simulations.

DOI:10.5506/APhysPolB.54.8-A3

[†] ly.nd@vlu.edu.vn
[‡] Corresponding author: duy.nguyen@vlu.edu.vn

1. Introduction

The rapid neutron capture (r-process) is believed to be the main nuclear process for the origin of heavy elements beyond iron [1, 2]. This astrophysical topic has been studied for many decades since the famous paper B^2FH was reported in 1957 [1] but the r-process has not been well understood so far [3–12]. In general, a combination of the beta-decay, neutron capture and its photodisintegration, beta-delay neutron emission and fission is thought to occur in this process [13–16]. The beta-decay shifts the reaction flows back to stability without changing the mass number A. The photodisintegration impedes the evolution via the neutron capture, which slow down the neutron enrichment for the neutron-rich isotopes. The neutron capture synthesizes the $A+1, A+2, \ldots$ isotopes to extend the nuclear chart to the neutron drip line. As a result, under conditions of $\rho_n > 10^{27}$ neutron·cm^{-3} and $T > 3$ GK [1, 17], the neutron capture dominates the β-decays to produce more neutron-rich nuclei until the (n,γ)–(γ,n) equilibrium is established. In such a scenario, there is a main competition between the β^--decay and neutron capture in the r-process [18–20]. Hence, the beta-decay half-life (or decay rate) is one of the most important factors for better understanding of nucleosynthesis via the r-process [14, 21–23]. For instance, it was found that a 45% increase in the ^{140}Sn half-life can lead to approximately 50% increase of the r-process abundance of the $A = 120$–135 isotopes [15]. If the half-life of ^{128}Ru is decreased by a factor of 10, the r-process abundance is increased by 100% for the isotopes around $A = 128$ but decreased by 30–50% for the nuclei with $A \geq 130$ [15]. Obviously, the uncertainty in the beta-decay rate significantly impacts the r-process abundance distribution. Unexpectedly, most half-lives are unknown or very uncertain for the r-process neutron-rich nuclei [24–27].

Recently, many theoretical [16, 28–30] and experimental attempts [25, 26, 31–33] have been conducted for more accurate half-lives of the extremely exotic nuclei. For instance, Panov *et al.* [16] employed the beta-strength functions based on the Finite Fermi-Systems Theory [34] to predict the half-life of the nuclei close to the neutron drip line. With this model, there is better accuracy of the prediction for the more neutron excess but a large uncertainty up to a factor of 10 still exists for the nuclei heavier than lead [16]. In another work by Möller *et al.* [48], the macroscopic–microscopic approach using the finite-range droplet model (FRDM) [28, 29] and quasiparticle random-phase approximation (QRPA) [35–38] was employed to estimate the nuclear masses and half-lives of more than 9300 isotopes from ^{16}O to ^{339}136. The comparison of the FRDM+QRPA results to available experimental data indicated that the half-lives have a large deviation, up to 2–3 orders of magnitude. Still, in a theoretical study, Borzov *et al.* [39] employed the Gamow–Teller + first-forbidden transitions and developed the

QRPA approximation to reduce the half-life uncertainty up to one order of magnitude for the neutron-rich isotopes far from stability. The results obtained by Borzov *et al.* were mostly by 30–60% shorter than those estimated by Suzuki *et al.* in Ref. [30] for the $Z = 66$–70 isotopes. With the help of the Radioactive Isotopes Beam Facility at RIKEN, the half-lives of many neutron-rich isotopes from ^{134}Sn to ^{155}La were measured with an uncertainty of up to 50% [26]. However, both calculations and experiments still have a large uncertainty, which is from a few factors to 3 orders of magnitude.

The semi-empirical approach is also an alternative to estimate the half-lives of the nuclei far from stability with an accuracy level similar to that in measurements, which is about one order of magnitude [21, 40–42]. For example, a simple semi-empirical formula as a power function of the binding-energy difference ΔE_{b} between the mother and daughter nuclei $T_{1/2} = \alpha(\Delta E_{\mathrm{b}})^{\beta}$ was proposed by Surman *et al.* [21], but it gives a large uncertainty in the half-life prediction due to the lack of microscopic corrections. In another study of Zhang *et al.* [41], a linear relation of the half-life in the logarithmic scale and nucleon (Z, N) numbers was proposed by using the Sargent law [43] and Fermi theory [44, 45]. By analyzing the dependence of the half-life on the decay energy and shell effect, the aforementioned relation was developed by adding a correction factor, which was described in terms of the Q-value and closed-(sub)shell numbers [41]. A more careful consideration for the impact of the Q-value, shell and pairing effects, nucleon numbers, and neutron excess on the half-life calculation was conducted in another work by Zhou *et al.* [42].

In our previous study [46], all the mentioned available semi-empirical formulae were evaluated to determine the uncertainty in the β-decay half-life prediction caused by the calculation methods. The influence of the beta-decay rates of the nuclei in the shell-closed region $N = 50, 82$, and 126 on the r-process abundance was in focus. In general, the empirical approaches depend on various impact factors, such as Q-value, shell and pairing effects, nucleon numbers, and neutron excess. Among these factors, nuclear mass or Q-value is the most important parameter for the half-life prediction. Unfortunately, nuclear masses of the extremely neutron-rich nuclei are unknown or very uncertain. The sensitivity of the half-life calculations to the uncertainty in the nuclear mass and/or in the other factors has not been well studied so far. Unfortunately, previous studies mostly focused on the investigations of the half-life theory instead of the sensitivity of the half-life to the impact factors. Hence, the effects of the uncertainty in the impact factors on the half-life prediction are still highly demanded.

In the present study, we focused on the influence of the mass uncertainty of the nuclei close to the dripline on the β-decay rates and, subsequently, on the isotopic r-process abundance. We re-estimated the half-lives of the exotic nuclei from Fe to La using the semi-empirical model proposed by Zhou *et al.* [42], which was considered a good method for the half-life estimations in previous studies [42, 46]. The nuclear mass (Q-value) including uncertainty in the newly evaluated experimental data AME2020 [47] and from the calculation based on the FRDM model [48] are used for the investigation. In other words, this work is studied to investigate the change in the β^--decay rate (and, subsequently, in the r-process calculation) due to the mass uncertainty.

The paper is constructed as follows. The theoretical method for the β-decay half-life and r-process simulation is described in Section 2. The half-lives of the extremely neutron-rich isotopes and r-process abundance calculated with different half-life and Q-value data sets are discussed in Section 3. The important results of the present study are summarized in Section 4.

2. Theoretical framework

2.1. β^--decay half-life calculation

Recently, many semi-empirical formulae [40–42] have been developed, since modern accelerator facilities enable scientists to access the nuclear properties of the exotic isotopes far from the stability through direct measurements. Using experimental data, semi-empirical models together with their fitting parameters have been improved. Among the models, a Q-value-dependent function of the β^--decay half-life proposed by Zhou *et al.* [42] emerges as a good candidate for predicting the half-life because both of newest experimental data and microscopic shell and pairing effects are taken into account in the formalism. Additionally, this model allows us to directly investigate the change in the half-life due to the experimental Q-value (or nuclear mass) uncertainty of isotopes. Therefore, the β-decay half-lives of extremely neutron-rich isotopes are determined using the Zhou semi-empirical formula ($F_{\rm Zh}$), which is given by [42]

$$F_{\rm Zh} : \ln T_{1/2} = a_6 + \left(\alpha^2 Z^2 - 5 - a_7 \frac{N-Z}{A}\right) \ln(Q - a_8\delta) + a_9\alpha^2 Z^2 + \frac{1}{3}\alpha^2 Z^2 \ln(A) - \alpha Z\pi + S(Z,N)\,, \quad (1)$$

where Z, N, and A are atomic, neutron, and mass numbers of β emitters, respectively; $\alpha = 1/137$ denotes the fine structure constant; and $\delta = (-1)^Z + (-1)^N$ is the even–odd staggering reflecting the pairing effects on the β-decay half-lives against Q-values, which can be determined based on the masses of the neutral mother ($M_{\rm m}$) and daughter ($M_{\rm d}$) atoms as $Q = M_{\rm m} - M_{\rm d}$.

The shell correction effect $S(Z,N)$ is calculated as

$$\begin{aligned} S(Z,N) \;=\; & a_1 \exp\left[-\frac{(Z-20)^2+(N-28)^2}{12}\right] \\ & + a_2 \exp\left[-\frac{(Z-38)^2+(N-50)^2}{43}\right] \\ & + a_3 \exp\left[-\frac{(Z-50)^2+(N-82)^2}{13}\right] \\ & + a_4 \exp\left[-\frac{(Z-58)^2+(N-82)^2}{24}\right] \\ & + a_5 \exp\left[-\frac{(Z-70)^2+(N-110)^2}{244}\right]. \end{aligned} \tag{2}$$

The parameters of $a_1 = 3.016$, $a_2 = 3.879$, $a_3 = 1.322$, $a_4 = 6.030$, $a_5 = 1.669$, $a_6 = 11.09$, $a_7 = 1.07$, $a_8 = -0.935$, and $a_9 = -5.398$ in the equation above were deduced by fitting all available experimental data to isotopes far from the β-decay stability [42].

In this study, the nuclear masses and Q-values, together with their uncertainties, are taken from the last updated mass database AME2020 [47]. If the data are not available in AME2020, the masses of isotopes are calculated using the model proposed by Myer *et al.* [49] with the uncertainties being assumed by 5%, which is mostly similar to the average uncertainties of experimental data.

2.2. r-process simulation

Although astrophysical sites for the r-process have not been well identified yet [50, 51], it is commonly believed that they are the stellar environments having extreme neutron density and temperature so that the nucleosynthesis can proceed through neutron-rich nuclei far away from the beta stability [2, 18, 52]. Several candidates, such as quark novae [53–56], neutron star mergers [57–62], and neutrino-driven winds [63–66] have been studied so far. Among them, the high-entropy neutron-driven winds, namely high-entropy wind (HEW), are thought to be a good astrophysical site for the main r-process [18, 52, 67–71]. In such a scenario, temperature, seed nuclei fraction, electron, matter, and neutron, *etc.* are changed due to an adiabatic expansion of the HEW bubble, leading to a change in the abundance of isotopes.

The entropy S, which is changed with the temperature T_9 (in GigaKelvin, 10^9 K) during the r-process evolution, is given by

$$S = \frac{11\pi^2 T_9^3}{45\rho} + \frac{\mu^2 T_9}{3\rho} + \frac{5}{2m_N} + \frac{1}{m_N}\ln\left(g_0 \frac{(2\pi m_N k T_9)^{3/2}}{n_n h^3}\right), \quad (3)$$

where μ is the chemical potential of the fully degenerate relativistic electrons; $m_N = 939.1$ MeV/c^2 is the neutron mass; and $g_0 = 2$ is the statistical weight of the neutron. The temperature depending on the expanding velocity $v_{\rm exp}$ (in km/s) of the HEW bubble is given by [91]

$$T_9(t) = T_9^{(0)} \times \frac{R_0}{R_0 + v_{\rm exp} t}, \quad (4)$$

where $T_9^{(0)}$ and R_0 (in km) are the temperature and bubble radius at the starting time $t = 0$ (in second), respectively. The matter density $\rho_5(t)$ (in the unit of 10^5 g/cm^3) varied by the temperature can be estimated as [91]

$$\rho_5(t) = 1.21 \frac{T_9^3}{S}\left[1 + \frac{7}{4}\frac{T_9^2}{T_9^2 + 5.3}\right]. \quad (5)$$

As mentioned in the previous section, a combination of the (n,γ) and (γ,n) reactions, β decays, and β-delayed neutron emission mainly occurs in the r-process [14, 72]. Accordingly, the rates of these processes are taken into the full network calculations for the abundance $Y(Z,A)$ of the (Z,A) isotope, which is given by [14]

$$\begin{aligned}\frac{{\rm d}Y(Z,A)}{{\rm d}t} &= Y(Z,A-1)\lambda_{n\gamma}^{(Z,A-1)} + Y(Z,A+1)\lambda_{\gamma n}^{(Z,A+1)} \\ &- Y(Z,A)\left[\lambda_{n\gamma}^{(Z,A)} + \lambda_{\gamma n}^{(Z,A)} + \lambda_{\beta}^{(Z,A)} + \lambda_{\beta n}^{(Z,A)} + \lambda_{\beta 2n}^{(Z,A)} + \lambda_{\beta 3n}^{(Z,A)}\right] \\ &+ Y(Z-1,A)\lambda_{\beta}^{(Z-1,A)} + Y(Z-1,A+1)\lambda_{\beta n}^{(Z-1,A+1)} \\ &+ Y(Z-1,A+2)\lambda_{\beta 2n}^{(Z-1,A+2)} + Y(Z-1,A+3)\lambda_{\beta 3n}^{(Z-1,A+3)}, \quad (6)\end{aligned}$$

where $\lambda_{n\gamma}$, $\lambda_{\gamma n}$, $\lambda_{\beta n}$, and $\lambda_{\beta xn}$ are the rates of the neutron capture (n,γ), photodisintegration (γ,n), β decay, and β decay followed by the emission of $x(=1,2,3)$ neutron(s), respectively.

For the r-process computations, the (n,γ) and (γ,n) reaction rates were calculated using the statistical Hauser–Feshbach model [73] with the help of the TALYS code [74]. The β-decay rates of the isotopes were out of the interest of the present study and β-delayed neutron-emission rates were taken from the calculation by Möller *et al.* in Ref. [28]. The beginning of the

r-process system is assumed to be in the $(n,\gamma) \rightleftarrows (\gamma,n)$ equilibrium with the initial conditions of temperature $T_9 = 3$ and neutron density $n_n = 10^{27}$ cm^{-3}. The initial conditions (*i.e.*, neutron density, neutron-to-seed ratio, temperature, mass density, *etc.*), which were calculated by Farouqi *et al.* [75], were used in the calculation. The β^--decay Q-values (with and without uncertainty) obtained from the newly evaluated experimental data in the AME2020 database [47] and those calculated using the FRDM model by Moller *et al.* [48] were used to investigate the uncertainty in the half-life prediction due to the mass uncertainty.

3. Results and discussion

We estimated the β-decay half-lives of 86 nuclei beyond the vicinity of $N = 50$ shell closure important for nuclear structure and astrophysics. Among these isotopes, 47 nuclides have no measured half-lives and the others have large uncertainties in experimental data [26, 27, 33]. Our calculations were separated into two data sets, which are based on the measured Q-values, AME2020 database [47] ($T_{1/2}^{\mathrm{AME}}$), and on those estimated using the FRDM method ($T_{1/2}^{\mathrm{FRDM}}$) in Ref. [48]. These calculations were compared to the predictions, in which the half-lives ($T_{1/2}^{\mathrm{FRDM+QRPA}}$) were calculated using the FRDM Q-values and the quasipartical random phase approximation (QRPA), performed by Möller *et al.* in Ref. [48]. The results are presented in Tables 1 and 2. It was found that the estimated half-lives based on the semi-empirical formula of all the investigated exotic isotopes are much shorter than 1 second, and are in the same order of millisecond similar to those predicted in Ref. [48] and measurements of [26, 27, 33]. The shortest and longest lifetimes can be observed to be about 9.5 and 457.5 ms for ^{78}Co and ^{90}Ge, respectively. On the other hand, the lifetimes of isotopes for each element are reduced by increasing the number of neutrons. Obviously, this phenomenon reflects the less stability of excessive-neutron isotopes [76, 77] since their binding energies per nucleon are decreasing by increasing the neutron number [47].

In Fig. 1, we show the deviations in the half-lives based on the semi-empirical model due to the β^--decay Q-value uncertainties obtained from the mass AME2020 database. It is clear that the half-lives are increased with decreasing Q-values. For instance, if the Q-value is reduced (or added) by about 6%, the half-life of the $^{127}_{45}$Rh nucleus will be enhanced (or reduced) by 35% (or 25%). Obviously, despite the same Q-value uncertainty, the rates of the half-life change ($T_{1/2}^{Q^*}/T_{1/2}^{Q}$) are different for the increasing or decreasing Q-value. This can be easily understood by the natural logarithmic relation described in Eq. (1). On the other hand, although the maximum

Table 1. Estimated β-decay half-lives (in milliseconds) of extremely neutron-rich nuclei from ^{75}Fe to ^{125}Ru, which were calculated using the semi-empirical model described in Eqs. (1)–(2) with the measured AME and FRDM β-decay energies, Q_β, taken from the AME2020 database [47] and Ref. [48], respectively. The half-lives calculated using the FRDM+QRPA method [48] and available experimental data [26, 27, 33] are provided in the two last columns for comparison. Notice that $T^{\rm AME}_{1/2-}$ and $T^{\rm AME}_{1/2+}$ (or $T^{\rm FRDM}_{1/2}$) denote the half-lives based on the Q-values of $Q-\Delta Q$ and $Q+\Delta Q$ (or $Q_{\rm FRDM}$), respectively.

$_Z X$	N	A	$[Q \pm \Delta Q]_{\rm AME}$	$Q_{\rm FRDM}$	$T^{\rm AME}_{1/2-}$	$T^{\rm AME}_{1/2}$	$T^{\rm AME}_{1/2+}$	$T^{\rm FRDM}_{1/2}$	Ref. [48]	Exp. [26, 27]
$_{26}$Fe	49	75	15.86±0.72	15.61	20.3	15.9	12.6	17.3	29.7	
$_{26}$Fe	50	76	15.07±0.78	14.48	14.1	10.9	8.6	13.2	21.3	
$_{27}$Co	51	78	19.56±0.81	20.15	12.2	9.5	7.5	8.0	5.9	
$_{28}$Ni	52	80	13.44±0.67	13.14	29.0	22.9	18.3	25.5	56.2	30±22
$_{28}$Ni	53	81	15.82±0.76	16.30	23.5	18.1	14.1	15.5	38.9	
$_{28}$Ni	54	82	15.01±0.89	14.84	15.9	12.0	9.1	12.6	29.4	
$_{29}$Cu	53	82	16.58±0.40	17.03	37.2	32.2	27.9	27.5	65.1	
$_{29}$Cu	54	83	15.90±0.58	16.11	23.6	19.4	16.0	18.1	25.5	
$_{30}$Zn	55	85	14.64±0.50	14.43	38.9	32.4	27.1	34.9	22.1	
$_{32}$Ge	54	86	9.56±0.44	8.74	298.3	243.0	199.5	358.4	161.5	221.6±11
$_{32}$Ge	57	89	13.49±0.50	13.31	62.6	51.4	42.4	55.1	15.2	
$_{32}$Ge	58	90	12.52±0.64	11.87	38.8	30.5	24.3	38.9	20.3	
$_{33}$As	55	88	13.43±0.20	12.81	261.9	239.1	218.7	318.7	78.8	270±150
$_{33}$As	56	89	12.46±0.30	11.76	136.6	120.3	106.3	162.7	58.9	
$_{33}$As	57	90	14.81±0.52	14.72	93.7	75.6	61.5	78.4	20.5	
$_{33}$As	58	91	14.08±0.59	13.22	48.5	38.8	31.3	53.9	28.5	
$_{33}$As	59	92	16.34±0.64	16.11	35.5	28.0	22.3	30.4	13.3	
$_{34}$Se	56	90	8.20±0.33	7.62	544.3	457.7	387.1	623.1	126.5	210±80
$_{34}$Se	57	91	10.53±0.43	10.53	326.5	262.8	213.3	262.8	36.5	270±50
$_{34}$Se	58	92	9.51±0.40	9.14	160.9	133.5	111.5	158.6	52.7	
$_{34}$Se	59	93	12.03±0.59	11.74	104.5	80.3	62.6	91.3	57.4	
$_{34}$Se	60	94	10.85±0.54	10.56	63.8	50.8	40.9	57.4	45.8	
$_{34}$Se	61	95	13.39±0.58	13.29	43.4	34.4	27.5	35.8	23.8	
$_{35}$Br	61	96	14.87±0.30	14.75	47.1	41.7	37.0	43.8	34.3	
$_{35}$Br	62	97	13.42±0.42	13.51	37.8	32.0	27.2	30.9	38.5	
$_{35}$Br	63	98	16.07±0.50	16.39	26.8	22.2	18.5	19.8	26.0	
$_{36}$Kr	65	101	13.99±0.50	13.64	27.0	22.3	18.6	25.5	12.9	
$_{36}$Kr	66	102	12.67±0.63	12.15	22.4	17.7	14.2	21.4	19.3	
$_{37}$Rb	66	103	14.12±0.45	13.53	24.7	20.8	17.7	26.0	15.9	
$_{37}$Rb	67	104	16.31±0.58	15.98	22.4	18.1	14.7	20.4	12.1	
$_{37}$Rb	68	105	15.03±0.75	14.61	18.7	14.3	11.1	16.6	10.8	
$_{37}$Rb	69	106	17.67±0.88	17.12	14.6	10.8	8.1	13.0	8.7	
$_{38}$Sr	65	103	11.18±0.20	10.91	80.1	72.9	66.5	82.8	31.8	53±10
$_{38}$Sr	68	106	11.49±0.78	10.65	36.6	26.7	19.9	37.5	34.9	21±8
$_{38}$Sr	69	107	13.72±0.86	13.15	32.0	22.8	16.6	28.5	26.9	
$_{38}$Sr	70	108	12.56±0.63	12.18	21.7	17.2	13.7	19.8	20.1	
$_{39}$Y	71	110	15.57±0.78	15.98	30.3	22.3	16.7	19.1	11.7	
$_{39}$Y	72	111	14.54±0.73	14.69	20.9	16.0	12.4	15.2	12.0	
$_{40}$Zr	72	112	11.65±0.76	10.92	31.9	23.6	17.7	31.5	42.7	43±21
$_{40}$Zr	73	113	13.87±0.50	13.42	24.6	20.3	16.8	24.1	26.3	
$_{40}$Zr	74	114	11.40±0.57	11.73	31.6	25.1	20.1	22.1	15.2	
$_{41}$Nb	75	116	15.98±0.58	15.47	22.4	18.0	14.6	21.8	12.9	
$_{41}$Nb	76	117	14.69±0.73	14.30	18.7	14.3	11.1	16.5	10.4	
$_{42}$Mo	77	119	13.59±0.58	12.90	26.7	21.3	17.1	27.9	21.6	
$_{43}$Tc	79	122	15.48±0.58	15.36	26.1	20.8	16.7	21.8	13.5	
$_{44}$Ru	81	125	13.46±0.58	12.16	28.7	22.8	18.3	38.7	33.0	

Table 2. Estimated β-decay half-lives (in milliseconds) of extremely neutron-rich nuclei from ^{127}Rh to ^{157}La, which were calculated using the semi-empirical model described in Eqs. (1)–(2) with the measured AME and FRDM β-decay energies, Q_β, taken from the AME2020 database [47] and Ref. [48], respectively. The half-lives calculated using the FRDM+QRPA method [48] and available experimental data [26, 27, 33] are provided in the two last columns for comparison. Notice that $T_{1/2-}^{\rm AME}$ and $T_{1/2+}^{\rm AME}$ (or $T_{1/2}^{\rm FRDM}$) denote the half-lives based on the Q-values of $Q-\Delta Q$ and $Q+\Delta Q$ (or $Q_{\rm FRDM}$), respectively.

$_Z X$	N	A	$[Q \pm \Delta Q]_{\rm AME}$	$Q_{\rm FRDM}$	$T_{1/2-}^{\rm AME}$	$T_{1/2}^{\rm AME}$	$T_{1/2+}^{\rm AME}$	$T_{1/2}^{\rm FRDM}$	Ref. [48]	Exp. [26, 27]
$_{45}$Rh	82	127	13.49±0.78	12.77	34.2	25.1	18.7	33.4	22.1	28±14
$_{45}$Rh	83	128	17.05±0.58	17.43	16.1	13.2	10.8	11.6	8.4	
$_{46}$Pd	84	130	13.17±0.52	12.50	18.4	15.3	12.8	19.4	68.5	
$_{46}$Pd	85	131	15.01±0.58	14.97	17.1	13.9	11.4	14.1	54.7	
$_{47}$Ag	85	132	16.07±0.50	16.85	26.2	21.7	18.1	16.5	27.7	30±14
$_{48}$Cd	86	134	12.51±0.36	11.65	22.4	19.6	17.3	27.0	150.0	65±15
$_{49}$In	88	137	14.32±0.50	14.11	19.3	16.1	13.4	17.3	40.1	70±40
$_{50}$Sn	88	138	9.14±0.50	10.07	84.0	66.1	52.6	43.5	226.3	148±9
$_{50}$Sn	89	139	10.74±0.57	12.57	90.5	68.3	52.3	30.3	162.1	120±38
$_{50}$Sn	90	140	9.90±0.67	11.12	54.8	40.5	30.4	24.3	68.2	
$_{51}$Sb	90	141	11.13±0.64	11.17	75.5	55.6	41.7	54.6	63.0	103±29
$_{51}$Sb	91	142	12.94±0.58	13.62	73.0	55.3	42.5	40.7	42.8	80±50
$_{52}$Te	88	140	7.33±0.02	6.86	202.7	200.6	198.5	262.4	338.8	360±21
$_{52}$Te	89	141	9.26±0.40	9.24	206.4	164.5	132.4	166.3	61.0	193±16
$_{52}$Te	90	142	8.25±0.50	7.83	122.9	94.7	73.9	117.8	120.8	147±8
$_{52}$Te	91	143	10.26±0.54	10.30	110.9	83.9	64.5	82.3	39.1	120±8
$_{52}$Te	92	144	9.11±0.50	8.98	73.6	57.9	46.0	61.5	54.8	93±60
$_{52}$Te	93	145	11.12±0.58	11.34	71.0	53.8	41.4	48.7	24.4	
$_{53}$I	89	142	10.43±0.01	10.65	272.2	271.2	270.2	237.7	73.7	235±11
$_{53}$I	90	143	9.41±0.20	9.37	162.5	145.5	130.7	148.8	128.4	182±8
$_{53}$I	91	144	11.54±0.40	11.64	146.1	117.6	95.5	111.5	49.3	94±8
$_{53}$I	92	145	10.36±0.50	10.39	102.9	79.8	62.6	78.6	76.2	89.7±9.3
$_{53}$I	93	146	12.42±0.30	12.73	83.4	71.9	62.2	61.9	36.6	94±26
$_{53}$I	94	147	11.20±0.36	11.36	62.6	52.9	45.0	49.2	48.1	
$_{54}$Xe	93	147	9.52±0.20	9.15	138.5	124.2	111.7	152.2	79.4	88±14
$_{54}$Xe	94	148	8.26±0.30	8.07	105.6	90.5	77.9	99.7	105.2	85±15
$_{54}$Xe	95	149	10.30±0.50	10.09	108.5	84.0	65.8	93.4	46.8	
$_{54}$Xe	96	150	9.18±0.50	9.06	75.4	59.4	47.3	62.9	53.5	
$_{55}$Cs	95	150	11.72±0.40	11.52	133.6	108.0	88.1	120.0	140.0	90±15
$_{55}$Cs	96	151	10.66±0.64	10.49	100.9	73.4	54.5	79.8	42.6	48±28
$_{56}$Ba	96	152	7.68±0.50	7.36	174.6	132.6	102.1	157.8	169.2	148±21
$_{56}$Ba	97	153	9.59±0.50	9.32	175.4	133.3	102.8	154.3	66.9	109±59
$_{56}$Ba	98	154	8.61±0.58	8.28	116.6	87.1	66.1	102.6	85.0	53±48
$_{57}$La	94	151	7.91±0.44	7.67	454.7	339.8	258.0	397.5	731.0	510±330
$_{57}$La	95	152	9.69±0.36	9.79	467.0	367.4	292.1	344.3	493.6	270±100
$_{57}$La	96	153	8.85±0.36	8.72	248.4	201.0	164.0	216.8	312.1	210±120
$_{57}$La	97	154	10.69±0.36	10.71	261.2	211.1	172.1	208.7	92.1	221±89
$_{57}$La	98	155	9.85±0.50	9.73	162.1	124.2	96.4	132.2	130.4	94±59
$_{57}$La	99	156	11.77±0.50	11.72	163.3	125.3	97.4	128.6	91.9	84±78
$_{57}$La	100	157	10.86±0.50	10.59	102.8	80.7	64.1	91.9	43.9	

value of the current Q-value uncertainties in measurements is only 7%, it can lead to large deviations, up to 40% in the estimated half-lives. It is observed that to achieve a better prediction (*i.e.*, less than 10%) for the half-life, the Q-value uncertainty is desired to be smaller than 2%. For example, with a deviation of 1.5% (about 200 keV) in the Q-value, the predicted half-life of $^{88}_{33}$As is varied by only 9%. Therefore, the accuracy of Q-values is important for the predictions of the β-decay half-lives of neutron-rich isotopes, especially for the semi-empirical model used in this work.

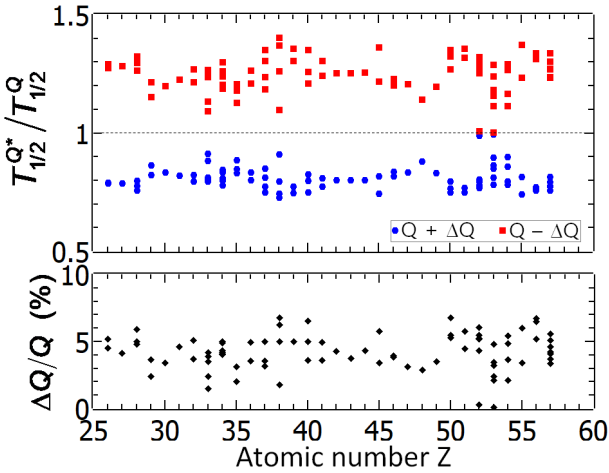

Fig. 1. Dependence of the half-lives on the β^--decay Q-values of isotopes. The upper panel shows the half-life deviations due to the Q-value uncertainties (lower panel). Notice that $T_{1/2}^{Q^*}$ denotes the half-lives $T_{1/2-}^{\mathrm{AME}}$ or $T_{1/2+}^{\mathrm{AME}}$ refers to Tables 1 and 2 calculated with $Q^* = Q - \Delta Q$ or $Q^* = Q + \Delta Q$, respectively.

To evaluate the importance of the mass model, we calculated the half-lives of the investigated isotopes using the same semi-empirical model but with different Q-value data sets, which are available from the AME2020 database (experimental data) and from calculations using the FRDM method in [48]. The differences among the β^--decay Q-values calculated using FRDM and measured data are shown in the lower panel of Fig. 2. It was found that the FRDM Q-values overestimate experimental data by up to 18% only for $^{138-140}_{50}$Sn but overall the FRDM calculation differs from the measurements by up to 10%. This deviation is much larger than that (7%) observed in measurements, as published in the AME2020 database. Besides, most of the FRDM Q-values underestimate those measured in laboratories. This discrepancy leads to a large deviation in the half-lives predicted using the semi-empirical approach, as can be seen in the upper panel of Fig. 2. For instance, with a Q-value difference of about 10%, the estimated half-life

of $^{125}_{44}$Ru is changed by 70%. Hence, the FRDM mass model needs to be improved for better predictions of nuclear masses and, subsequently, β-decay half-lives of isotopes far from the stability.

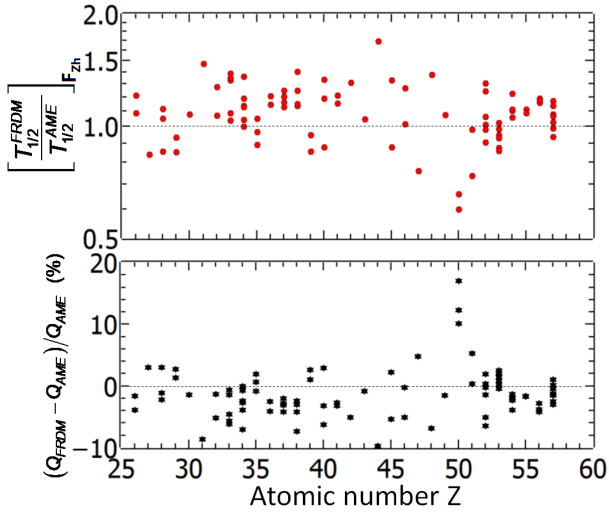

Fig. 2. Lower panel: The difference between the FRDM and measured Q-values and upper panel: A comparison between the estimated half-lives calculated using the FRDM and AME2020 Q-values ($T_{1/2}^{\mathrm{FRDM}}$ and $T_{1/2}^{\mathrm{AME}}$, respectively).

By using the semi-empirical formula together with the FRDM Q-values (namely FRDM+F_{Zh}), we calculated the half-lives ($T_{1/2}^{\mathrm{FRDM}}$) of the investigated isotopes and compared them to those predicted by using the FRDM+QRPA method [35–38] in Ref. [48] to consider the impact of theoretical models on the half-life predictions. As can be seen in panel (A) of Fig. 3, the FRDM+QRPA half-lives mostly differ by up to a factor of about 6 from those based on the FRDM+F_{Zh} method. In general, the FRDM+QRPA approach overestimates the FRDM+F_{Zh} method for Z = 26–29 and 46–50 isotopes, and *vice versa* for Z = 30–45 and 51–57. This difference can be understood by unavoidable uncertainties of microscopic parameters in the QRPA calculations and the inability of the F_{Zh} expression to capture all the variability in the half-lives of the isotopes under study. It should be noted that the Gamow–Teller strength taken into the FRDM+QRPA half-life calculation in Ref. [48] is very sensitive to the deformation parameter, β_2, [78–80] which is unknown or very uncertain for the investigated isotopes. In the study by Möller *et al.* [48] of the FRDM+QRPA half-lives, the deformation parameters were calculated using the FRDM method [29]. Additionally, the shell correction terms, $S(Z, N)$, calculated using the FRDM and semi-empirical F_{Zh} (see Eq. (2)) approaches are also very different from each other.

The large discrepancy between the FRDM+QRPA and FRDM+$F_{\rm Zh}$ results indicate that the β-decay half-lives are still very uncertain due to different calculation methods. In other words, together with precise nuclear mass, a reliable model for predicting β^--decay half-lives of extremely neutron-rich nuclei are still highly demanded.

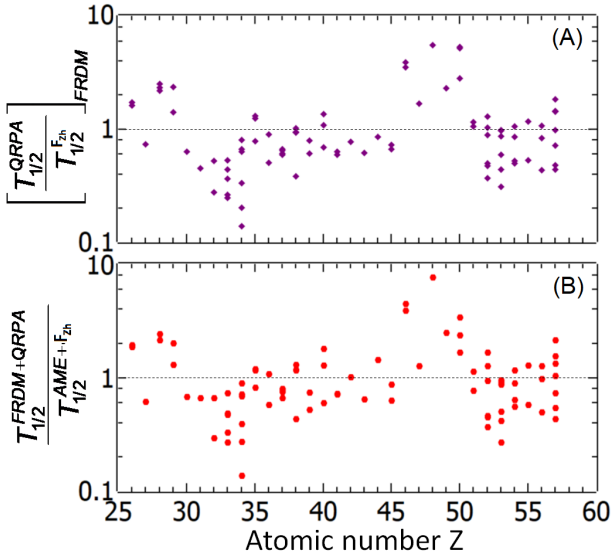

Fig. 3. Panel A: The ratios of the QRPA half-lives ($T_{1/2}^{\rm QRPA}$) in Ref. [48] to those based on the FRDM Q-values and semi-empirical formula ($T_{1/2}^{F_{\rm Zh}}$) in the present study. Panel B: A comparison of the half-lives calculated using semi-empirical approach with AME2020 Q-values ($T_{1/2}^{\rm AME+F_{Zh}}$) and those ($T_{1/2}^{\rm FRDM+QRPA}$) taken from the previous study [48]. The dotted lines are to guide the eyes.

As can be seen in panel (B) of Fig. 3, the half-lives calculated in the present study ($T_{1/2}^{\rm AME+F_{Zh}}$) are up to one order of magnitude different from those ($T_{1/2}^{\rm FRDM+QRPA}$) obtained from Ref. [48]. Since the predicted half-lives strongly depend on the Q-values and microscopic parameters in calculations as discussed above, it can be understood that this large uncertainty is rising from the differences in both nuclear mass models and calculation methods. Together with the results in panel (A), we can conclude that the uncertainty in the predictions of the β-decay half-lives is still large, about one order of magnitude, due to the uncertainty in nuclear mass and difference in theoretical models.

Figure 4 shows a comparison of the calculated half-lives based on the semi-empirical and QRPA approaches in two cases of the experimental and FRDM Q-values to those measured in laboratories. Table 3 presents the aver-

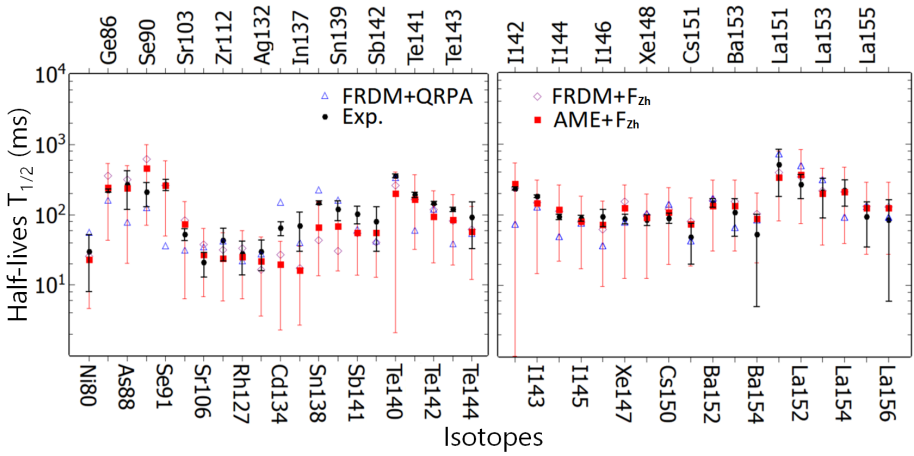

Fig. 4. Half-lives (in logarithmic scale) of 39 nuclei calculated using the semi-empirical formula in Eq. (1) with Q-values obtained from the AME2020 database (red filled squares) and FRDM (purple opened diamonds) calculation [48] are compared to those estimated by using the FRDM+QRPA method in Ref. [48] (blue opened triangles) and available experimental data (black solid dots). The red thin (or black thick) lines indicate the half-life uncertainties due to the measured Q-value deviations (or the errors in available experimental half-lives of the investigated nuclei).

Table 3. Deviations between β^--decay half-lives calculated using semi-empirical formula with the AME2020 (AME+$F_{\rm Zh}$) and FRDM (FRDM+$F_{\rm Zh}$) Q-values and available experimental data of the investigated nuclei [26, 27, 33].

	AME+$F_{\rm Zh}$	FRDM+$F_{\rm Zh}$	FRDM+QRPA
$\bar{\delta}$	0.058	0.034	0.097
rms	0.205	0.239	0.284

age ($\bar{\delta}$) and standard (rms) deviations, which are deduced using Eqs. (7)–(8), between the calculated and measured half-lives. It is clear that, by considering the measured Q-value uncertainties, the deviations in the estimated half-lives are much larger than the measured half-life uncertainties. However in general, the experimental data fall in the AME+$F_{\rm Zh}$ results if the Q-value uncertainty is taken into the calculation. This again reflects the important role of the precise Q-values in the lifetime estimation for exotic isotopes. On the other hand, with the smallest standard deviation (rms = 0.205), the AME+$F_{\rm Zh}$ approach is the most reliable model for estimating the β^--decay

half-lives of extremely neutron-rich isotopes beyond ^{75}Fe. The results also indicate that the FRDM+$F_{\rm Zh}$ approach ($\bar{\delta} = 0.034$, rms $= 0.239$) is better than the FRDM+QRPA method ($\bar{\delta} = 0.097$, rms $= 0.284$) in predictions of the half-lives

$$\bar{\delta} = \frac{1}{39}\sum_{k=1}^{39}\left|\log\frac{T_{1/2i}}{T_{1/2}^{\rm exp}}\right|, \tag{7}$$

$$\text{rms} = \sqrt{\sum_{i=1}^{39}\frac{\left|\log T_{1/2i} - \log T_{1/2}^{\rm exp}\right|^2}{39}}. \tag{8}$$

As mentioned in Section 2, together with the neutron capture process, the β^--decay influences the reaction flows and abundance of isotopes in the r-process [14, 81, 82]. Hence, we examined the deviations in isotopic abundances due to the uncertainty, which is caused by the mass (or β^--decay Q-value) uncertainty, in the estimated β^--decay half-lives of the investigated nuclei. Since the high entropy wind (HEW) surrounding a proto-neutron star in collapses of supernovae is believed to be the r-process scenario for the synthesis of nuclei beyond Fe [18, 52, 67–71], we calculated the r-process abundance under the typical HEW conditions [75] at $S = 400$ (k_B/baryon). The initial conditions of temperature, electron fraction, and expansion velocity of HEW bubbles were assumed to be $T = 3 \times 10^9$ K, $Y_e = 0.3$, and $v = 7500$ km/s, respectively, for the calculations. Notice that these conditions were well determined by Farouqi *et al.* in Ref. [75].

Figure 5 shows the abundances of isotopes with $A = 80$–260, which were calculated by using the β-decay rates ($\lambda_\beta = \ln 2/T_{1/2}$ s^{-1}) based on different Q-values (AME2020 [47] and FRDM calculations [48]) of the investigated nuclei. The results show that the second ($A \approx 130$), rare-earth-element pygmy ($A = 140$–180), and third $A \approx 195$ peaks can be produced in the HEW conditions at $S = 400$. Regardless of the magnitude, these peaks are in good agreement with those obtained in the solar system [83] and r-process pattern [70]. This is the evidence for the main contribution of the r-process in the solar system at the $A \approx 130$, $A = 140$–180, and $A \approx 195$ peaks. Notice that the difference of about 3–4 orders of magnitude between the abundance in the solar system and that in the present study is the common problem in the r-process calculations [52, 70, 84–86], which is caused by unavoidably ambiguous factors in the astrophysical sites of the r-process (*i.e.*, entropy, matter density, expansion velocity, *etc.*) and in the nuclear process (*i.e.*, neutron capture rates, beta-delay neutron emission probability, fission probability, *etc.*) as reported in previous studies [14, 26, 82, 87]. On the other hand, the third peak at $A \approx 195$ in the calculation of the present

study is slightly shifted to lower mass as compared to that in the pattern. This phenomenon can be understood by the unsatisfactory feature of the astrophysical trajectory employed to produce the abundance as reported in Ref. [70]. Additionally, in contrast to the previous study by Otsuki *et al.* [70], the beta-delay neutron emission and lower neutron-to-seed conditions, which strongly impact the distribution of isotopes in peaks [52, 88, 89], were taken in the calculation in the present study.

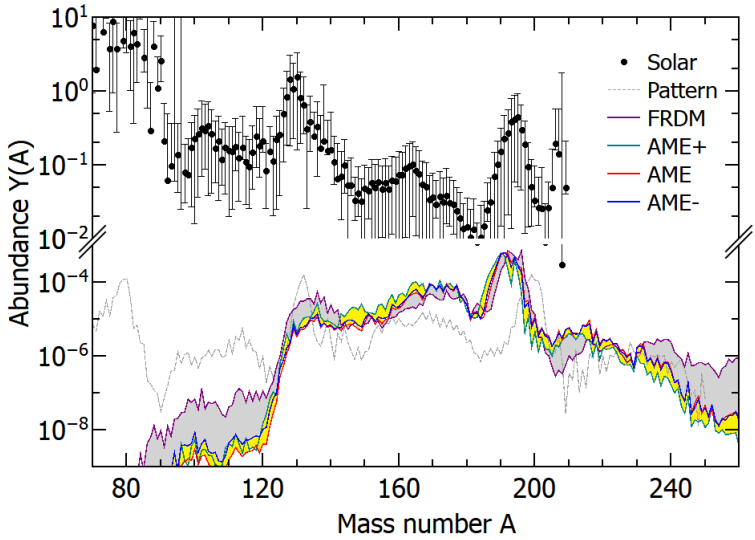

Fig. 5. The r-process abundance (in logarithmic scale) in the HEW environment at a high entropy $S = 400$ calculated with various beta-decay rate estimations and Q-values. The shaded yellow (or gray) areas indicate the difference among the abundances calculated using $Q^* = Q \pm \Delta Q$ and Q in the AME2020 mass database (or Q_{FRDM} and Q) values. The dashed gray curves denote the r-process pattern calculated by Otsuki *et al.* [70]. The solar-system abundance (black dots) is adapted from Ref. [83].

The impact of the β^--decay Q-values on the r-process abundance is shown in Fig. 6. Panels (A), (B), and (C) show the differences between the abundance based on $Q^* = Q - \Delta Q$ ($Y_{\mathrm{AME}-}$), $Q^* = Q + \Delta Q$ ($Y_{\mathrm{AME}+}$), and FRDM (Y_{FRDM}) mass data, respectively, and that (Y_{AME}) based on the mean values Q in the AME2020 database. It was found that an uncertainty of 40% in the half-life due to the 7% deviation in the Q-value (see Fig. 1) leads to a large change, up to one order of magnitude, in the r-process abundance. The abundance $Y_{\mathrm{AME}-}$ overestimates Y_{AME} for the isotopes ranging in $A = 80$–130, while they are mostly the same for the nuclei with $A \geq 130$. On the other hand, with the 10% of Q-value difference between

the FRDM model and AME2020, the half-life was changed up to a factor of about 2, leading to a large deviation of up to two orders of magnitude in the isotopic abundance (panel (C)).

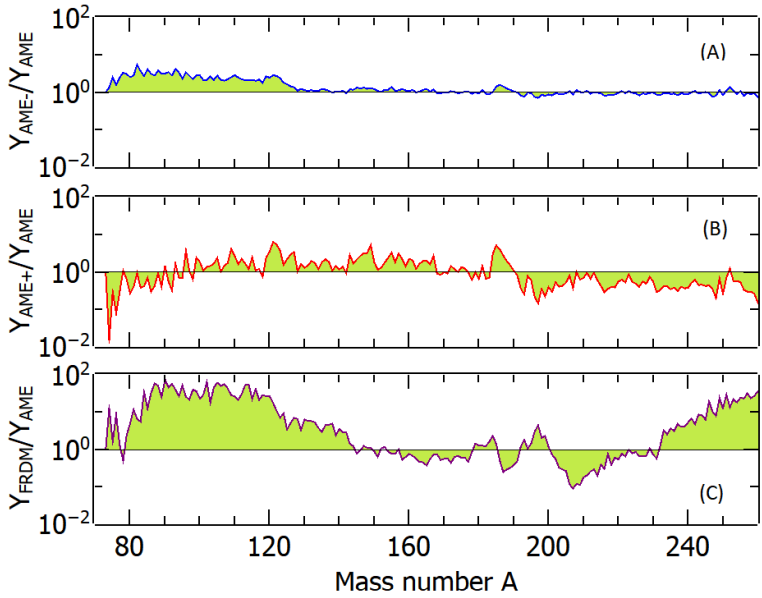

Fig. 6. Ratios Y_{Q^*}/Y_Q of the abundances calculated using $Q^* = Q + \Delta Q$ ($Y_{\mathrm{AME+}}$), $Q^* = Q - \Delta Q$ ($Y_{\mathrm{AME+}}$), and Q_{FRDM} (Y_{FRDM}) to those (Y_{AME}) based on the Q-values. The horizontal dashed lines are to guide the eyes when ratios are equal to 1.

We found that the β^--decay rates of the nuclei from Fe ($N \approx 50$, $A \approx 80$) to Sb ($N \approx 82$, $A \approx 130$) strongly impact the abundances in the range of $A = 80$–130. For instance, the higher decay rates (shorter half-lives) estimated using $Q^* = Q - \Delta Q$ and Q_{FRDM} of these nuclei lead to the higher contribution of the $A = 70$–130 isotopes as compared to the abundance (Y_{AME}) based on the Q, see panels (A) and (C) of Fig. 6. In contrast, the slower decay rates (longer half-lives) calculated using $Q^* = Q + \Delta Q$ results in the lower distribution, as can be seen in panel (B). This result can be understood by the dominance in the competition between the decay and the neutron capture. The fast decay shifts the reaction path towards the stability without changing the mass number A, leading to the enrichment of the isotopes in the same mass region [90, 91]. On the other hand, the slight change in the $A = 140$–180 mass range indicates that the abundance of the isotopes in the rare-earth-element pygmy peak is not sensitive to the decay rates of the extremely exotic nuclei close to the neutron drip line. However, slower decay rates based on Q_{FRDM} of these isotopes impact the enhancement of the nuclei heavier than bismuth ($A > 210$), as can be seen

in panel (C). This phenomenon is a result of the combination of beta decay, neutron capture, beta-delay neutron emission, and fission of heavy nuclei in the r-process, as well described in Refs. [13–16].

The results discussed above indicate that precise mass measurements for the extremely neutron-rich nuclei close to the neutron drip line are necessary for better understanding of the nuclear structure, decay rates, and astrophysical calculations. By considering the half-life (and its uncertainty), we find that it is difficult to measure the precise masses of the ^{78}Co, ^{106}Rb, and ^{128}Rh isotopes by using a technique with a measuring time longer than 10 ms. All the isotopes of interest can be measured by using the Multi-Reflection Time-of-Flight method [92, 93], which has a few milliseconds of the measuring timescale.

4. Conclusion

We examined the β^--decay half-lives of the extremely exotic nuclei close to the neutron drip line. The half-lives were calculated using a reliable semi-empirical formula ($F_{\rm Zh}$) with different β^--decay Q-values, which were evaluated in the newly updated mass database, AME2020 (with and without uncertainty), and calculated using the finite-range droplet macroscopic (FRDM) model. We confirmed that the half-lives based on the AME+$F_{\rm Zh}$ model are in good agreement (rms = 0.205) with available experimental data and better than those calculated using the FRDM+$F_{\rm Zh}$ and FRDM+QRPA models *for the isotopes ranging from Fe to La.* The uncertainty in the half-life prediction is mostly similar to that in the measurements. To achieve a deviation of less than 10% in the half-life prediction, the Q-value uncertainty is required to be smaller than 2%. On the other hand, a mass uncertainty of 10% can result in a large uncertainty, up to two orders of magnitude, in the r-process abundance, especially for the isotopes ranging in $A = 80$–130 and $A > 210$ mass regions. However, the abundance of the isotopes in the rare-earth-element pygmy peak ($A = 140$–180) is just slightly impacted by the decay rates of the nuclei close to the neutron drip line. Hence, precise mass measurements for the isotopes of interest are highly recommended. The estimated half-lives are also very important to consider the mass measurement techniques. The present study provides useful information for further studies on the neutron-rich isotopes and nucleosynthesis via the r-process.

The financial support from the Van Lang University for this study is acknowledged. L.H. Khiem is supported by the International Centre of Physics at the Institute of Physics (grant No. ICP.2023.04) and the Vietnam Academy of Science and Technology (grant No. NCVCC05.01/22-23).

REFERENCES

[1] E.M. Burbidge, G.R. Burbidge, W.A. Fowler, F. Hoyle, «Synthesis of the Elements in Stars», *Rev. Mod. Phys.* **29**, 547 (1957).

[2] J.J. Cowan, F.-K. Thieleman, J.W. Truran, «The R-process and nucleochronology», *Phys. Rep.* **208**, 267 (1991).

[3] G.J. Wasserburg, M. Busso, R. Gallino, «Abundances of Actinides and Short-lived Nonactinides in the Interstellar Medium: Diverse Supernova Sources for the r-Processes», *Astrophys. J.* **466**, L109 (1996).

[4] F. Kappeler, «The origin of the heavy elements: The s process», *Prog. Part. Nucl. Phys.* **43**, 419 (1999).

[5] Y.-Z. Qian, G.J. Wasserburg, «Where, oh where has the r-process gone?», *Phys. Rep.* **442**, 237 (2007).

[6] S. Shibagaki *et al.*, «Relative Contributions of the Weak, Main, and Fission-recycling r-process», *Astrophys. J.* **816**, 79 (2016).

[7] D. Kasen *et al.*, «Origin of the heavy elements in binary neutron-star mergers from a gravitational-wave event», *Nature (London)* **551**, 80 (2017).

[8] K. Kawaguchi, M. Shibata, M. Tanaka, «Radiative Transfer Simulation for the Optical and Near-infrared Electromagnetic Counterparts to GW170817», *Astrophys. J.* **865**, L21 (2018).

[9] Y.-L. Zhu *et al.*, «Californium-254 and Kilonova Light Curves», *Astrophys. J.* **863**, L23 (2018).

[10] M.-R. Wu, J. Barnes, G. Martínez-Pinedo, B.D. Metzger, «Fingerprints of Heavy-Element Nucleosynthesis in the Late-Time Lightcurves of Kilonovae», *Phys. Rev. Lett.* **122**, 062701 (2019).

[11] M.M. Kasliwal *et al.*, «Spitzer mid-infrared detections of neutron star merger GW170817 suggests synthesis of the heaviest elements», *Mon. Not. R. Astron. Soc. Lett.* **510**, L7 (2021).

[12] D. Watson *et al.*, «Identification of strontium in the merger of two neutron stars», *Nature* **574**, 497 (2019).

[13] T. Marketin, L. Huther, G. Martínez-Pinedo, «Large-scale evaluation of β-decay rates of r-process nuclei with the inclusion of first-forbidden transitions», *Phys. Rev. C* **93**, 025805 (2016).

[14] M. Mumpower *et al.*, «Sensitivity studies for the main process: β-decay rates», *AIP Advances* **4**, 041009 (2014).

[15] M.R. Mumpower *et al.*, «The impact of individual nuclear properties on r-process nucleosynthesis», *Prog. Part. Nucl. Phys.* **86**, 86 (2016).

[16] I.V. Panov *et al.*, «Beta-decay half-lives for the r-process nuclei», *Nucl. Phys. A* **947**, 1 (2016).

[17] A.G.W. Cameron, «Nuclear Reactions in Stars and Nucleogenesis», *Publ. Astron. Soc. Pac.* **69**, 201 (1957).

[18] S. Wanajo, T. Kajino, G.J. Mathews, K. Otsuki, «The r-Process in Neutrino-driven Winds from Nascent, "Compact" Neutron Stars of Core-Collapse Supernovae», *Astrophys. J.* **554**, 578 (2001).

[19] S. Wanajo *et al.*, «The r-Process in the Neutrino Winds of Core-Collapse Supernovae and U–Th Cosmochronology», *Astrophys. J.* **577**, 853 (2002).

[20] J.B. Blake, D.N. Schramm, «A Possible Alternative to the R-Process», *Astrophys. J.* **209**, 846 (1976).

[21] R. Surman, J. Engel, J.R. Bennett, B.S. Meyer, «Source of the Rare-Earth Element Peak in r-Process Nucleosynthesis», *Phys. Rev. Lett.* **79**, 1809 (1997).

[22] D. Martin, A. Arcones, W. Nazarewicz, E. Olsen, «Impact of Nuclear Mass Uncertainties on the r Process», *Phys. Rev. Lett.* **116**, 121101 (2016).

[23] I.V. Panov, Yu.S. Lutostansky, «Nucleosynthesis-Rate Dependence of Abundances of Nuclei Produced in the r-Process», *Phys. Atom. Nucl.* **83**, 613 (2020).

[24] Z.M. Niu *et al.*, «Predictions of nuclear β-decay half-lives with machine learning and their impact on r-process nucleosynthesis», *Phys. Rev. C* **99**, 064307 (2019).

[25] J. Wu *et al.*, «94 β-Decay Half-Lives of Neutron-Rich to $_{55}$Cs to $_{67}$Ho: Experimental Feedback and Evaluation of the r-Process Rare-Earth Peak Formation», *Phys. Rev. Lett.* **118**, 072701 (2017); *Erratum ibid.* **120**, 139902 (2018).

[26] J. Wu *et al.*, «β-decay half-lives of 55 neutron-rich isotopes beyond the $N = 82$ shell gap», *Phys. Rev. C* **101**, 042801(R) (2020).

[27] F.G. Kondev *et al.*, «The NUBASE2020 evaluation of nuclear physics properties», *Chinese Phys. C* **45**, 030001 (2021).

[28] P. Möller, J.R. Nix, W.D. Myers, W.J. Swiatecki, «Nuclear Ground-State Masses and Deformations», *Atom. Data Nucl. Data Tables* **59**, 185 (1995).

[29] P. Möller, A.J. Sierk, T. Ichikawa, H. Sagawa, «Nuclear ground-state masses and deformations: FRDM(2012)», *Atom. Data Nucl. Data Tables* **109–110**, 1 (2016).

[30] T. Suzuki, T. Yoshida, T. Kajino, T. Otsuka, «β decays of isotones with neutron magic number of $N = 126$ and r-process nucleosynthesis», *Phys. Rev. C* **85**, 015802 (2012).

[31] U.C. Bergmann *et al.*, «Beta-decay properties of the neutron-rich $^{94-99}$Kr and $^{142-147}$Xe isotopes», *Nucl. Phys. A* **714**, 21 (2003).

[32] G. Lorusso *et al.*, «β-Decay Half-Lives of 110 Neutron-Rich Nuclei across the $N = 82$ Shell Gap: Implications for the Mechanism and Universality of the Astrophysical r Process», *Phys. Rev. Lett.* **114**, 192501 (2015).

[33] G. Audi *et al.*, «The NUBASE2016 evaluation of nuclear properties», *Chinese Phys. C* **41**, 030001 (2017).

[34] H.V. Klapdor *et al.*, «The beta strength function and the astrophysical site of the r-process», *Z. Phys. A* **299**, 213 (1981).

[35] J. Krumlinde, P. Möller, «Calculation of Gamow–Teller β-strength functions in the rubidium region in the RPA approximation with Nilsson-model wave functions», *Nucl. Phys. A* **417**, 419 (1984).

[36] P. Möller, B. Pfeiffer, K.-L. Kratz, «New calculations of gross β-decay properties for astrophysical applications: Speeding-up the classical r process», *Phys. Rev. C* **67**, 055802 (2003).

[37] H. Homma *et al.*, «Systematic study of nuclear β decay», *Phys. Rev. C* **54**, 2972 (1996).

[38] K. Muto, E. Bender, T. Oda, H.V. Klapdor-Kleingrothaus, «Proton–neutron quasiparticle RPA with separable Gamow–Teller forces», *Z. Phys. A* **341**, 407 (1992).

[39] I.N. Borzov, «Gamow–Teller and first-forbidden decays near the r-process paths at $N = 50, 82$, and 126», *Phys. Rev. C* **67**, 025802 (2003).

[40] Z. Zhang, Z. Ren, «New exponential law of β^+-decay half-lives of nuclei far from β-stable line», *Phys. Rev. C* **73**, 014305 (2006).

[41] Z. Zhang, Z. Ren, Q. Zhi, Q. Zheng, «Systematics of β^--decay half-lives of nuclei far from the β-stable line», *J. Phys. G: Nucl. Part. Phys.* **34**, 2611 (2007).

[42] Y. Zhou *et al.*, «Empirical formula for β^--decay half-lives of r-process nuclei», *Sci. China Phys. Mech. Astron.* **60**, 082012 (2017).

[43] B.W. Sargent, «The maximum energy of the β-Rays from uranium X and other bodies», *Proc. R. Soc. A* **139**, 659 (1933).

[44] E. Fermi, «Versuch einer Theorie der β-Strahlen. I», *Z. Phys.* **88**, 161 (1934).

[45] T.H.R. Skyrme, «Theory of Beta-decay», *Prog. Nucl. Phys.* **1**, 115 (1950).

[46] N.K. Uyen, K.Y. Chae, N.N. Duy, N.D. Ly, «Beta-decay half-lives of the extremely neutron-rich nuclei in the closed-shell $N = 50, 82, 126$ groups», *J. Phys. G: Nucl. Part. Phys.* **49**, 025201 (2022).

[47] M. Wang *et al.*, «The AME 2020 atomic mass evaluation (II). Tables, graphs and references», *Chinese Phys. C* **45**, 030003 (2021).

[48] P. Möller, M.R. Mumpower, T. Kawan, W.D. Myers, «Nuclear properties for astrophysical and radioactive-ion-beam applications (II)», *Atom. Data Nucl. Data Tables* **125**, 1 (2019).

[49] W.D. Myers, W.J. Swiatecki, «Nuclear masses and deformations», *Nucl. Phys.* **81**, 1 (1966).

[50] M. Arnould, S. Goriely, K. Takahashi, «The r-process of stellar nucleosynthesis: Astrophysics and nuclear physics achievements and mysteries», *Phys. Rep.* **450**, 97 (2007).

[51] F.-K. Thielemann *et al.*, «What are the astrophysical sites for the r-process and the production of heavy elements?», *Prog. Part. Nucl. Phys.* **66**, 346 (2011).

[52] S.E. Woosley *et al.*, «The r-process and neutrino-heated supernova ejecta», *Astrophys. J.* **433**, 229 (1994).

[53] N. Nurmamat *et al.*, «Quark novae: An alternative channel for the formation of isolated millisecond pulsars», *J. Astrophys. Astron.* **40**, 32 (2019).

[54] R. Ouyed, J. Dey, M. Dey, «Quark-Nova», *Astron. Astrophys.* **390**, L39 (2002).

[55] D. Leahy, R. Ouyed, «Supernova SN2006gy as a first ever Quark Nova?», *Mon. Not. R. Astron. Soc.* **387**, 1193 (2008).

[56] P. Jaikumar, B.S. Meyer, K. Otsuki, R. Ouyed, «Nucleosynthesis in neutron-rich ejecta from quark-novae», *Astron. Astrophys.* **471**, 227 (2007).

[57] B.J. Shappee *et al.*, «Early spectra of the gravitational wave source GW170817: Evolution of a neutron star merger», *Science* **358**, 1574 (2017).

[58] M.R. Drout *et al.*, «Light curves of the neutron star merger GW170817/SSS17a: Implications for r-process nucleosynthesis», *Science* **358**, 1570 (2017).

[59] S. Wanajo *et al.*, «Production of All the r-process Nuclides in the Dynamical Ejecta of Neutron Star Mergers», *Astrophys. J.* **789**, L39 (2014).

[60] D. Kasen, N.R. Badnell, J. Barnes, «Opacities and Spectra of the r-process Ejecta from Neutron Star Mergers», *Astrophys. J.* **774**, 25 (2013).

[61] B.D. Metzger, «Electromagnetic counterparts of compact object mergers powered by the radioactive decay of r-process nuclei», *Mon. Not. R. Astron. Soc.* **406**, 2650 (2010).

[62] Y.-Z. Qian, «Supernovae versus Neutron Star Mergers as the Major r-Process Sources», *Astrophys. J.* **534**, L67 (2000).

[63] S. Fujibayashi, T. Yoshida, Y. Sekiguchi, «Nucleosynthesis in Neutrino-driven Winds in Hypernovae», *Astrophys. J.* **810**, 115 (2015).

[64] A. Perego *et al.*, «Neutrino-driven winds from neutron star merger remnants», *Mon. Not. R. Astron. Soc.* **443**, 3134 (2014).

[65] A. Arcones, F.-K. Thielemann, «Neutrino-driven wind simulations and nucleosynthesis of heavy elements», *J. Phys. G: Nucl. Part. Phys.* **40**, 013201 (2013).

[66] T. Fischer *et al.*, «Protoneutron star evolution and the neutrino-driven wind in general relativistic neutrino radiation hydrodynamics simulations», *Astron. Astrophys.* **517**, A80 (2010).

[67] K. Takahashi, J. Witti, H.-Th. Janka, «Nucleosynthesis in neutrino-driven winds from protoneutron stars II. The r-process», *Astron. Astrophys.* **286**, 857 (1994).

[68] Y.-Z. Qian, S.E. Woosley, «Nucleosynthesis in Neutrino-driven Winds. I. The Physical Conditions», *Astrophys. J.* **471**, 331 (1996).

[69] C.Y. Cardall, G.M. Fuller, «General Relativistic Effects in the Neutrino-driven Wind and r-Process Nucleosynthesis», *Astrophys. J.* **486**, L111 (1997).

[70] K. Otsuki, H. Tagoshi, T. Kajino, S. Wanajo, «General Relativistic Effects on Neutrino-driven Winds from Young, Hot Neutron Stars and r-Process Nucleosynthesis», *Astrophys. J.* **533**, 424 (2000).

[71] T.A. Thompson, A. Burrows, B.S. Meyer, «The Physics of Proto–Neutron Star Winds: Implications for r-Process Nucleosynthesis», *Astrophys. J.* **562**, 887 (2001).

[72] M.R. Mumpower *et al.*, «Estimation of $M1$ scissors mode strength for deformed nuclei in the medium- to heavy-mass region by statistical Hauser–Feshbach model calculations», *Phys. Rev. C* **96**, 024612 (2017).

[73] T. Rauscher, F.-K. Thielemann, «Astrophysical Reaction Rates From Statistical Model Calculations», *At. Data Nucl. Data Tables* **75**, 1 (2000).

[74] S. Goriely, S. Hilaire, A.J. Koning, «Improved predictions of nuclear reaction rates with the TALYS reaction code for astrophysical applications», *Astron. Astrophys.* **487**, 767 (2008).

[75] K. Farouqi *et al.*, «Charged-particle and Neutron-capture Processes in the High-entropy Wind of Core-collapse Supernovae», *Astrophys. J.* **712**, 1359 (2010).

[76] M.P. Fewell, «The atomic nuclide with the highest mean binding energy», *Am. J. Phys.* **63**, 653 (1995).

[77] N.R. Sree Harsha, «The tightly bound nuclei in the liquid drop model», *Eur. J. Phys.* **39**, 035802 (2018).

[78] E. Ha, M.-K. Cheoun, «Shell evolution of $N = 20$ nuclei and Gamow–Teller strengths of ^{30,32,34}Mg with deformed quasiparticle random-phase approximation», *Phys. Rev. C* **88**, 017603 (2013).

[79] E. Ha, M-K. Cheoun, «Nuclear Structure of ^{12,14}Be Within Deformed Quasi-Particle Random Phase Approximation (DQRPA)», *Few-Body Syst.* **54**, 1389 (2013).

[80] P. Sarriguren, E. Moya de Guerra, A. Escuderos, «decay in odd-A and even–even proton-rich Kr isotopes», *Phys. Rev. C* **64**, 064306 (2001).

[81] K.-L. Kratz, K. Farouqi, B. Pfeiffer, «Nuclear-data input to the classical r-process: The case of β-decay properties», *AIP Conf. Proc.* **1852**, 030001 (2017).

[82] J.J. Cowan *et al.*, «Origin of the heaviest elements: The rapid neutron-capture process», *Rev. Mod. Phys.* **93**, 015002 (2021).

[83] S. Goriely, «Uncertainties in the solar system r-abundance distribution», *Astron. Astrophys.* **342**, 881 (1999).

[84] B. Zhao, S.Q. Zhang, «The r-process with the Newly Developed High-precision Mass Model WS4», *Astrophys. J.* **874**, 5 (2019).

[85] B.S. Meyer *et al.*, «R-process nucleosynthesis in the high-entropy supernova bubble», *Astrophys. J.* **399**, 656 (1992).

[86] K.-L. Kratz, K. Farouqi, P. Möller, «A High-entropy-wind r-process Study Based on Nuclear-structure Quantities from the New Finite-range Droplet Model FRDM(2012)», *Astrophys. J.* **792**, 6 (2014).

[87] Z.M. Niu *et al.*, «β-decay half-lives of neutron-rich nuclei and matter flow in the r-process», *Phys. Lett. B* **723**, 172 (2013).

[88] E.A. McCutchan *et al.*, «Improving systematic predictions of β-delayed neutron emission probabilities», *Phys. Rev. C* **86**, 041305(R) (2012).

[89] C. Domingo-Pardo *et al.*, «Approaching the precursor nuclei of the third r-process peak with RIBs», *J. Phys.: Conf. Ser.* **665**, 012045 (2016).

[90] K.-L. Kratz, «Nuclear Physics Constraints to Bring the Astrophysical R-Process to the "Waiting Point"», in: G. Klare (Ed.) «Cosmic Chemistry. Reviews in Modern Astronomy», Vol. 1, *Springer*, Berlin, Heidelberg 1988.

[91] M. Kostka *et al.*, «The r-Java 2.0 code: nuclear physics», *Astron. Astrophys.* **568**, A97 (2014).

[92] M.P. Reiter *et al.*, «Improved beam diagnostics and optimization at ISAC via TITAN's MR-TOF-MS», *Nucl. Instrum. Methods Phys. Res. B* **463**, 431 (2020).

[93] P. Schury *et al.*, «Improving wide-band mass measurements in a multi-reflection time-of-flight mass spectrograph by usage of a concomitant measurement scheme», *Int. J. Mass Spectrom.* **433**, 40 (2018).